



Circadian regulator NR1D2 regulates glioblastoma cell proliferation and motility

Min Yu¹ · Wenjing Li¹ · Qianqian Wang¹ · Yan Wang² · Fei Lu¹ 

Received: 8 November 2017 / Revised: 23 April 2018 / Accepted: 24 April 2018
© Macmillan Publishers Limited, part of Springer Nature 2018

Abstract

Nuclear receptor NR1D2 is originally characterized as the repressor of genes involved in circadian rhythm. Recently, it is documented that NR1D2 is overexpressed in various cancers. However, the pathways and biological functions that NR1D2 involved in cancers remain poorly understood. Here, we reported that NR1D2 was abundant in human glioblastoma (GBM) tissue and cell lines but not primary human astrocytes. Silencing of NR1D2 changed the morphology of GBM cells, inhibited cell proliferation and motility, whereas had no effects on apoptosis. Importantly, based on RNA-seq and ChIP assay, we identified receptor tyrosine kinase AXL as a new transcriptional target of NR1D2 in GBM cells. AXL mediated partially the regulatory effects of NR1D2 on PI3K/AKT axis and promoted proliferation, migration, and invasion of GBM cells. Besides, NR1D2 knockdown remarkably impaired the maturation of focal adhesion and assembly of F-actin, along with downregulated p-FAK, and proteins involved in actin nucleation and polymerization (p-Rac1/Cdc42, WAVE and PFN2). Moreover, NR1D2 had more targets other than AXL to regulate epithelial-to-mesenchymal transition and cell motility in GBM cells. Altogether, our findings uncover a GBM-promoting role of NR1D2 and provide the rationale for targeting NR1D2 as a potential therapeutic approach.

Introduction

Glioblastoma (GBM) is one of the most aggressive malignancies of central nervous system disease due to its highly invasive feature that impedes the surgical removal of all tumor cells, which results in the inevitable relapse, and patients generally have a poor prognosis with median overall survival of 12–18 months, 2-year survival of 15–20%, and 5-year survival of 3–5% [1, 2]. In the last 10 years, many new drugs and therapeutic approaches have been evaluated, such as bevacizumab, cilengitide,

temsirolimus, rindopepimut, including PD-1 antibody nivolumab, but encouraging outcomes are not observed in newly diagnosed or recurrent glioblastoma [2–8]. To date, the standard therapy for newly diagnosed glioblastoma is still maximal safe surgical resection, followed by radiation therapy and temozolomide concurrent with and adjuvant to radiotherapy. It is imperative that novel approaches and targets for therapy are explored to improve patient prognosis and eventually overcome this fatal disease.

Based on bioinformatics analysis, the molecular profile of most GBM samples is more mesenchymal than epithelial [9]. Epithelial-to-mesenchymal transition (EMT) renders cancer cells the invasive properties and results in cancer progression and metastasis. EMT is regulated by several signaling pathways (Stat3, NF- κ B, MAPK, PI3K/AKT) and is strongly associated with GBM malignancy [10–12]. EMT is enhanced during irradiation [12, 13] and temozolomide or carmustine treatment [14, 15], emphasizing a prominent role in GBM recurrence and therapy-resistance.

AXL, a member of the TAM (TYRO3-AXL-MER) family of receptor tyrosine kinases (RTKs), is overexpressed and activated in a multitude of cancers, including human GBM [16–18]. AXL also has positive-correlation with the EMT phenotype, poor prognosis, increased

Electronic supplementary material The online version of this article (<https://doi.org/10.1038/s41388-018-0319-8>) contains supplementary material, which is available to authorized users.

✉ Fei Lu
lufei@pkusz.edu.cn

- ¹ State Key Laboratory of Chemical Oncogenomics, Key Laboratory of Chemical Genomics, Peking University Shenzhen Graduate School, Shenzhen 518055, China
- ² Department of Cardiology, Qingdao Municipal Hospital, Qingdao University, Qingdao 266011, China

metastasis, and drug resistance [19–24]. AXL is generally activated by its ligand growth arrest specific 6 (Gas6) [25]. Although constitutive activation mutants of AXL are rarely found in cancer, it can be dimerized in Gas6-independent manner when the RTK is overexpressed [26]. Targeting AXL in different model systems with specific small molecule inhibitors or antibodies alone or in combination with other drugs can lead to inactivation of AXL-mediated signaling pathways, regained drug sensitivity, and improved therapeutic efficacy [19, 24, 27–29]. Although these findings implicate AXL to be an emerging therapeutic target for advanced disease, the mechanism how AXL is overexpressed in tumors remains largely unknown.

NR1D2 (nuclear receptor subfamily 1 group D member 2, also known as ERV-REB β) is a variant of NR1D1 and generally characterized as a repressor [30, 31]. In addition to be a repressor, NR1D2 can activate Srebp-1c in skeletal muscle cells [32]. It is documented that NR1D1 and NR1D2 have redundant functions in regulating circadian rhythm, metabolism and inflammatory response [33–37]. But it seems they diverge in cancer cells. NR1D2 is the major variant in various human cancer cells, while NR1D1 is more abundant in normal tissues [38]. However, the pathways and biological functions that NR1D2 involved in cancers remain unclear.

In this study, we identified AXL as a novel transcriptional target of NR1D2 in GBM cells. This might establish a link between NR1D2 and AXL overexpression in glioblastoma. We observed that knockdown of NR1D2 inhibited proliferation and motility of GBM cells. Transcriptome analysis demonstrated the involvement of NR1D2 in focal adhesion signaling pathway (RTK/PI3K/AKT and FAK). Indeed, knockdown of NR1D2 repressed AXL/PI3K/AKT and FAK signaling pathways. Thus, we uncover the biological role of NR1D2 in gliomagenesis, reveal a complex and critical signaling network mediated by NR1D2 in GBM cells, and identify NR1D2 as a novel anti-cancer therapeutic target.

Results

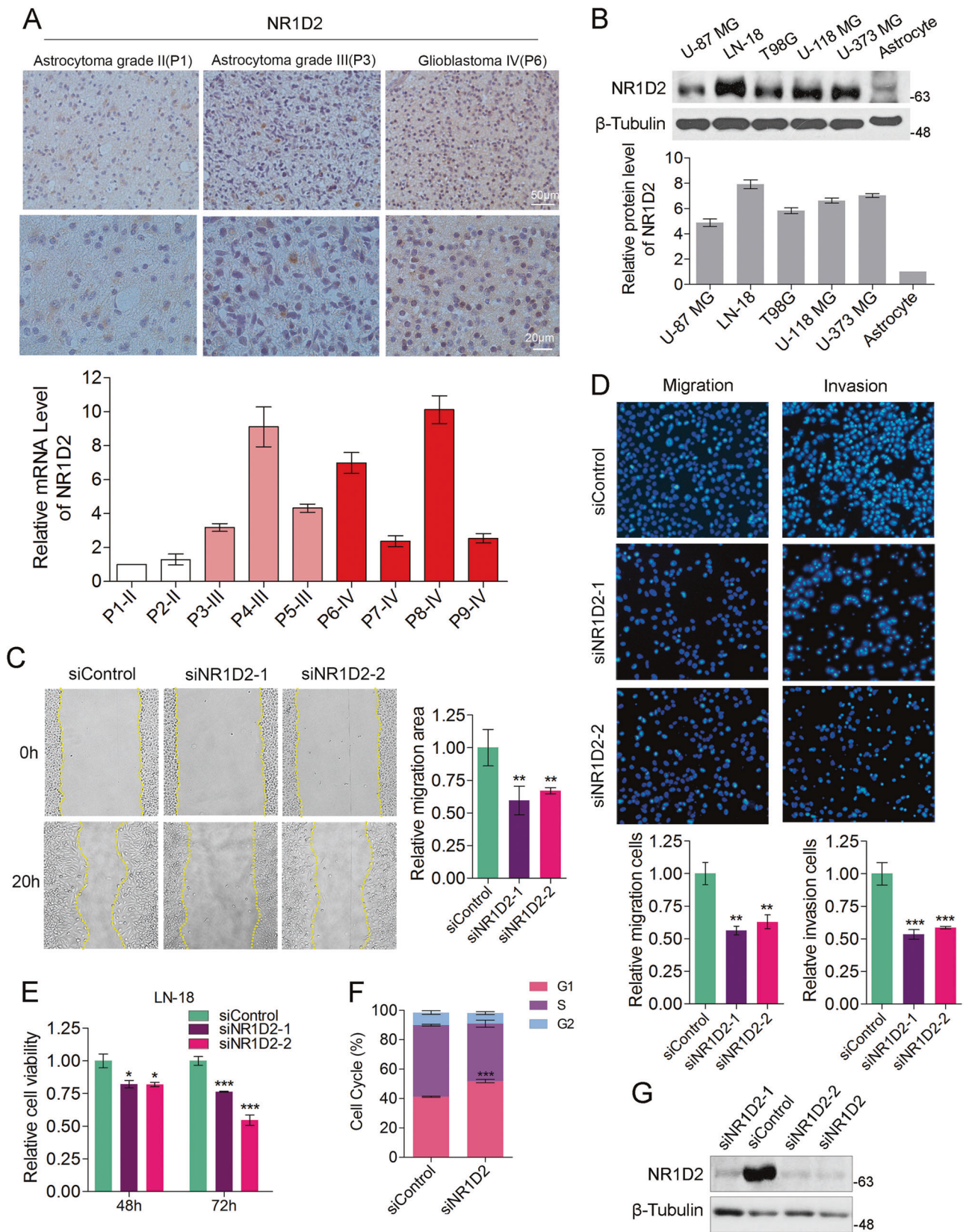
NR1D2 is highly expressed in human glioblastoma

To explore the functions of circadian regulator NR1D2 in glioblastoma (GBM), the most frequent malignant brain tumor, NR1D2 expression was detected in human glioma specimens of different grades by immunohistochemistry staining and Quantitative reverse transcription PCR (RT-qPCR). NR1D2 was moderately expressed and mainly localized in the cytoplasm in low-grade gliomas (astrocytoma grade II). Whereas in astrocytoma grade III

and especially in glioblastoma grade IV, the protein level of NR1D2 was much higher, and showed a strong nuclear staining (Fig. 1a upper panel). It was consistent with the mRNA level of NR1D2 in human glioma specimens (Fig. 1a lower panel). Similarly, the protein level of NR1D2 was abundant in human GBM cell lines U-87 MG, LN-18, T98G, U-118 MG, and U-373 MG, but lower in primary human astrocytes (Fig. 1b). The data imply that NR1D2 is highly expressed in glioma and may positively correlate with a malignant phenotype.

Knockdown of NR1D2 inhibits migration, invasion, and proliferation of glioblastoma cells

To investigate the role of NR1D2 in GBM, we silenced NR1D2 using gene-specific siRNAs in LN-18, T98G, U-118 MG cells and primary human astrocytes (HA). To rule out off-target effects of siRNAs, we designed two pairs of siRNAs targeting to NR1D2. Verified that each pair of siRNAs has the similar efficacy and phenotype on LN-18 cells, we used the siRNA mixture in subsequent experiments and other cell lines. Firstly, we noticed a morphological change that the cells were smaller and rounded after NR1D2 knockdown (NR1D2-KD) in LN-18 (Supplementary Fig. S1A), U-118 MG, and T98G cells (Fig. S1B). Then we asked whether cells underwent apoptosis when cells were rounded up following treatment with NR1D2 siRNAs. We performed apoptosis assay by Annexin V/PI staining and discovered that inhibition of NR1D2 did not increase the population of apoptosis cells, compared with siControl in GBM cells (Supplementary Fig. S2F). Unexpectedly, the shape of HA was not affected by NR1D2-KD (Supplementary Fig. S1C). It implied that NR1D2 might have a specific function in cancer cells. Next, we found that the migration of LN-18, T98G and U-118 MG cells was slowed down post depletion of NR1D2, which was confirmed by wound healing and transwell assays (Fig. 1c, d, and Supplementary Fig. S2C, D). Besides, the capability of invasion was also impaired in NR1D2-KD LN-18 cells in Matrigel coated transwell systems (Fig. 1d). Additionally, the cell viability was reduced (Fig. 1e and Supplementary Fig. S2A) and the population of cells in G1 phase was increased (Fig. 1f) post knockdown of NR1D2, whereas the cell viability of HA was not affected by NR1D2 depletion (Supplementary Fig. S2E). The efficacy of siRNAs targeting to NR1D2 was verified by western blotting (Fig. 1g and Supplementary Fig. S2B). Altogether, our data state that NR1D2 plays a specific role in glioblastoma.



◀ **Fig. 1** NR1D2 is required for the proliferation and migration of LN-18 cells. **a** NR1D2 was highly expressed in glioblastoma. Upper panel: The different grades of human glioma sections were immunohistochemically stained by anti-NR1D2 antibody. Scale bar: 50 or 20 μm . Lower panel: The mRNA level of NR1D2 was measured by RT-qPCR in human glioma sections. P1–P9 indicated patient 1 to patient 9. **b** NR1D2 was highly expressed in glioblastoma cells than primary human astrocytes. Upper panel: The protein levels of NR1D2 were determined by western blotting in glioblastoma cells U-87 MG, LN-18, T98G, U-118 MG, U-373 MG, and primary human astrocytes. Lower panel: The relative protein levels of NR1D2 were densitometric quantified by Image J from triplicates. **c** Loss of NR1D2 impaired migration of LN-18 cells. Wound healing assay was performed on NR1D2 knockdown (NR1D2-KD) LN-18 cells. Relative scratch covered area was quantified by Image J from four areas. **d** Representative images of transwell-based cell migration and invasion of NR1D2-KD LN-18 cells. Matrigel was coated on the bottom of the well as the basement membrane matrix for invasion assay. The migration and invasion cell numbers were quantified by Image J in 12 random fields from three independent experiments. **e** Relative cell viability of NR1D2-KD cells were measured by MTT assay. **f** Flow cytometric analysis (FCAS) displayed that NR1D2 knockdown increased the population of G1 phase LN-18 cells. **g** The efficacy of siRNAs was validated by western blotting using anti-NR1D2 antibody. SiNR1D2 was the mixture of siNR1D2-1 and siNR1D2-2. Histograms in this figure were shown as means \pm SD (standard derivation). Bars denoted SD. * $P < 0.05$; ** $P < 0.01$; *** $P < 0.001$

AXL is highly expressed in glioblastoma cells and is a target of NR1D2

To further investigate where NR1D2 targeted to and which signaling pathway NR1D2 was involved in, we silenced NR1D2 using gene-specific siRNAs in LN-18 cells. RNA-seq was performed to identify differentially expressed genes (DEGs) post loss of NR1D2. There were 3760 DEGs in NR1D2-KD cells compared with the parallel control, of which 1871 upregulated and 1889 downregulated (Fig. 2a, Supplementary Tables S1 and S2). We were especially interested in identifying NR1D2 targets that could be molecular targets for GBM therapy, including kinases, secreted factors, or receptors. Based on these criteria, we found that the receptor tyrosine kinase (RTK) AXL was reduced ~ 2.5 fold in NR1D2-KD cells (Fig. 2b). Meanwhile, previously studies indicate that AXL is over-expressed in glioblastoma [16, 39]. We examined the expression of AXL in GBM cell lines and the results showed that AXL was highly expressed in GBM cell lines compared with primary human astrocytes (Fig. 2c).

To validate AXL being a NR1D2 regulated gene in GBM cells, we examined AXL expression when NR1D2 was knockdown. The protein level of AXL was remarkably decreased in NR1D2-KD GBM cells compared with siControl cells, whereas it was not affected in NR1D2-KD human astrocytes (HA) (Fig. 2d and Supplementary Fig. S3B). It is well established that AXL is a RTK that localizes on the cell membrane. We then asked whether NR1D2

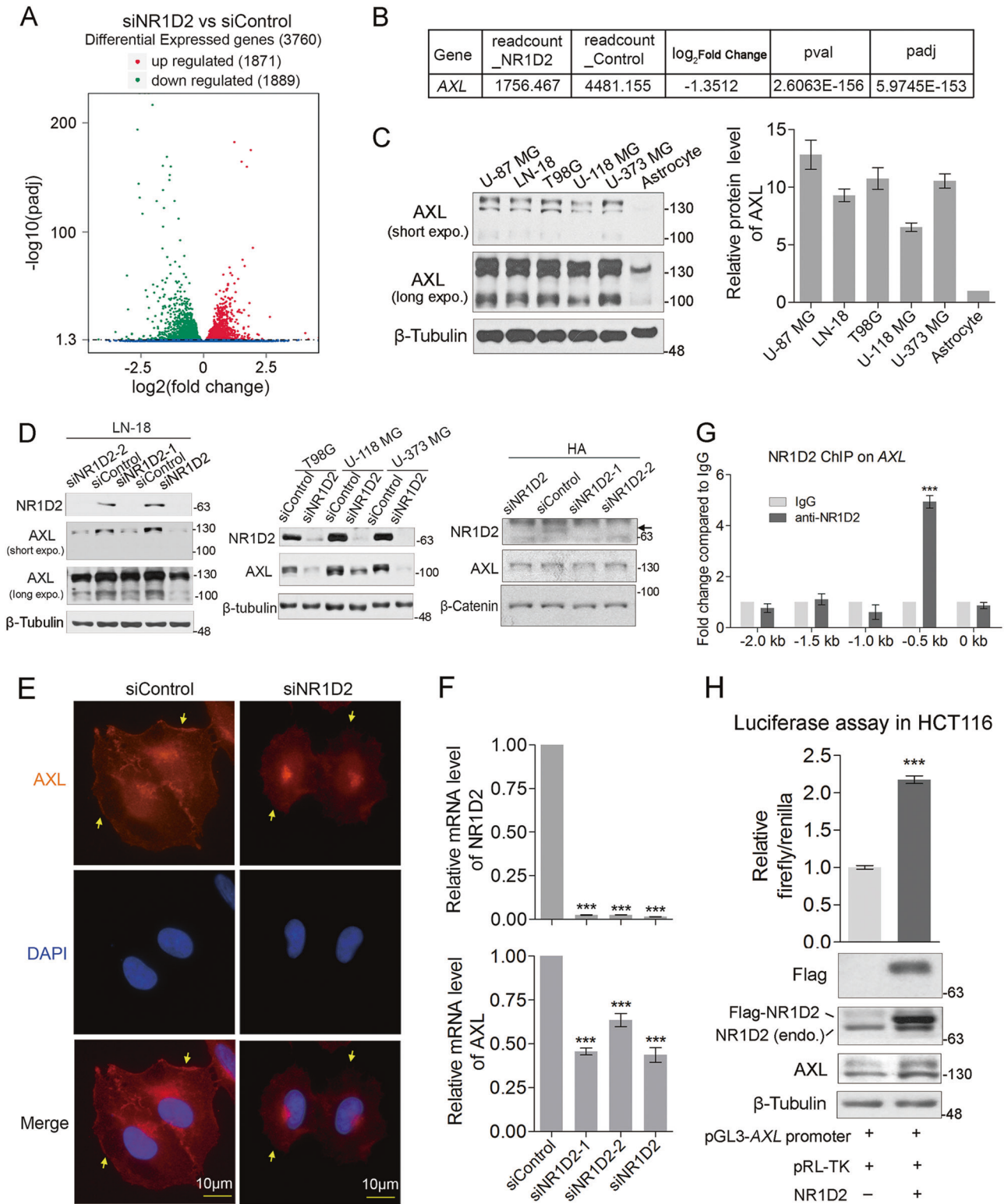
regulated membrane localization of AXL. Immunofluorescence was carried out in LN-18 and T98G cells. We found that knockdown of NR1D2 obviously reduced the cytomembrane localization of AXL (Fig. 2e and Supplementary Fig. S3A). Taken together, these findings demonstrate that NR1D2 regulates AXL expression and cytomembrane localization in GBM cells.

Since NR1D2 is a nuclear receptor, we further confirmed that AXL was transcriptional regulated by NR1D2 using RT-qPCR in LN-18 cells (Fig. 2f). The mRNA levels of NR1D2 and AXL were significantly reduced in NR1D2-KD cells compared with siControl cells (Fig. 2f). To determine if AXL was a direct target of NR1D2, we performed ChIP assay in LN-18 cells, and DNA fragments bound by endogenous NR1D2 were immunoprecipitated by anti-NR1D2 antibody. Quantitative PCR analysis stated that NR1D2 bound to AXL promoter at the position from -304 bp to -467 bp (Fig. 2g). To test whether NR1D2 can activate AXL in vivo, we performed luciferase assays in HCT116 cells using the fragment from -177 bp to -600 bp of the AXL promoter, since it was extremely difficult to transfect expression plasmids into GBM cell lines. The results illustrated that expression of full-length NR1D2 was sufficient to activate AXL promoter in HCT116 cells (Fig. 2h). These data demonstrate that NR1D2 directly binds to and activates AXL.

Inactivation of AXL inhibits the migration, invasion, and proliferation of glioblastoma cells

As a direct target of NR1D2 and having the similar expression profile with NR1D2 in GBM cells, AXL had the predictable overlapping function with NR1D2. AXL was abolished using gene-specific siRNAs in GBM cells, and then wound healing and transwell assays were applied to determine the migration ability of LN-18 cells. As showed in Fig. 3a, b, knockdown of AXL suppressed LN-18 cells migration, as well as invasion. Consistently, silencing of AXL inhibited T98G and U-118 MG cells migration in wound healing and transwell assays (Supplementary Fig. S4A, B).

Besides, to examine the role of AXL on cell proliferation, we performed flow cytometry assay to probe newly synthesized DNA with the incorporation of EdU in LN-18 cells. The results suggested that knockdown of AXL inhibited cell proliferation (Fig. 3c). Moreover, MTT assay performed in T98G cells confirmed that silencing of AXL was capable of inhibiting cell proliferation (Supplementary Fig. S4C). And the population of apoptosis cells was slightly increased when AXL was silenced (Supplementary Fig. S4E). The efficacy of siRNAs targeting to AXL was verified by western blotting (Fig. 3D and Supplementary Fig. S4D). Altogether, our data indicate that AXL is essential for the proliferation or migration of GBM cells.



NR1D2 may regulate cell proliferation through AXL/PI3K/AKT signaling pathway in glioblastoma cells

Next, we sought to find signaling pathway that involved in siNR1D2-mediated inhibition on GBM cells. We performed

KEGG pathway enrichment analysis on RNA-seq data and obtained 20 enrichment pathways in the DEGs (Fig. 4a). Among them, focal adhesion ($P = 1.79E-05$) had strong positive-correlation with NR1D2 (Fig. 4a). Gene-set enrichment analysis (GSEA) confirmed the positive-

◀ **Fig. 2** *AXL* is a new target of NR1D2. **a** Volcanic map showed overall distribution of DEGs in NR1D2-KD LN-18 cells compared with siControl, which was analyzed by RNA-seq. DEGs, differentially expressed genes. **b** Results from the RNA-seq stated the mRNA level change of *AXL* in NR1D2-KD LN-18 cells compared with siControl. **c** The protein levels of *AXL* in human GBM cell lines and normal astrocytes. Relative protein levels were quantified by Image J from triplicates. **d** The protein levels of *AXL* were downregulated in NR1D2-KD glioblastoma cells but not astrocytes. SiNR1D2 was the mixture of siNR1D2-1 and siNR1D2-2. The quantification of *AXL* protein level was shown in Supplementary Fig. S3B. **e** Cell membrane localization of *AXL* was reduced in NR1D2-KD LN-18 cells, which was detected by immunostaining using anti-*AXL* antibody (yellow arrowhead indicated). Scale bar: 10 μ m. **f** Knockdown of NR1D2 transcriptional inhibited the expression of *AXL*. The mRNA levels of *NR1D2* and *AXL* were examined by quantitative RT-PCR. **g** NR1D2 associated with *AXL* promoter region. ChIP assay was performed using anti-NR1D2 antibody, and rabbit IgG was taken as negative control. **h** Dual-Luciferase reporter assays stated the activation function of NR1D2 on *AXL* promoter. Exogenous NR1D2 (Flag) and endogenous NR1D2 were verified by western blotting using anti-Flag and anti-NR1D2 antibodies. Histograms in this figure were shown as means \pm SD (standard derivation). Bars denoted SD. *** $P < 0.001$

correlation between NR1D2 and focal adhesion pathway in NR1D2-KD LN-18 cells (Fig. 4b). RTK/PI3K/AKT axis is one of the focal adhesion signaling pathways and plays important roles in cell proliferation and motility (Fig. S5). Since *AXL* is a RTK, we asked whether NR1D2 involved in RTK/PI3K/AKT axis mediated by *AXL*. As expected, silencing of NR1D2 inhibited *AXL* expression and reduced phosphorylation of *AXL* (Y779), as well as phosphorylated PI3K-P85(Y458)/P55(Y119) and phosphorylated AKT (S472/3) in LN-18, U-118 MG, and T98G cells (Fig. 4c and Supplementary Fig. S6A, B). The similar results were obtained when *AXL* was knockdown (Fig. 4d and Supplementary Fig. S6D), whereas silencing of *AXL* did not affect the expression of NR1D2 (Fig. 4d). Interestingly, the phosphorylation of PI3K and AKT in HA was not changed when NR1D2 was knockdown (Supplementary Fig. S6C). The data indicate that NR1D2 and *AXL* may be in the same pathway and *AXL* is the downstream target of NR1D2 in GBM cells.

To figure out that *AXL* played a direct or indirect role in this pathway, we carried out a rescue assay using *AXL*-expressing adenoviruses system (customer pAdm-*AXL*, ViGene Biosciences). Interestingly, expression of ectopic *AXL* compensated the decreased phosphorylation of PI3K (P85 and P55) and AKT (Fig. 4e) and restored the cell proliferation in NR1D2-knockdown LN-18 cells (Fig. 4f). The data state that NR1D2 regulates GBM cells proliferation through *AXL*/PI3K/AKT pathway.

NR1D2 has more targets other than *AXL* to regulate EMT of glioblastoma cells

Besides promoting the proliferation of cells, *AXL* also stimulated migration and invasion of NR1D2-knockdown LN-18 cells (Fig. 5a). As we known, EMT confers cancer cells migratory and invasive properties. Thus, we asked whether NR1D2 regulated EMT of GBM cells. Indeed, among the DEGs, an enrichment of genes related to EMT was observed, including well established EMT-markers *CDH1*, *SNAI1*, *ZEB2*, *SNAI2*, et al. (Fig. 5b). Since loss of E-cadherin is considered to be a fundamental event in EMT, we examined the expression of E-cadherin and its transcription regulators post NR1D2 knockdown. As expected, the protein level of E-cadherin (the epithelial marker) was obviously increased, meanwhile its transcription regulator Slug (also named *SNAI2*) was significantly decreased, whereas other transcription factor Snail1 (also named *SNAI1*) was not affected in NR1D2-KD LN-18 cells. (Fig. 5c and Supplementary Fig. S7A). To our surprise, except for LN-18 cells, the expression of E-cadherin was undetectable in U-118 MG cells (Fig. 5c, d), as well as in HA (Supplementary Fig. S7B). The expression of Slug was not affected by NR1D2 silencing in HA (Supplementary Fig. S7B). Besides, the mRNA level of *MMP9* was decreased in NR1D2-KD GBM cells measured by RT-qPCR (Supplementary Fig. S7C). Collectively, these results suggest that knockdown of NR1D2 may suppress EMT of glioblastoma and subsequent metastasis.

As the downstream target of NR1D2, *AXL* phenocopied the effects of NR1D2 on EMT of GBM cells. The protein level of E-cadherin was upregulated and the expression of Slug and *MMP9* was downregulated after *AXL* knockdown (Fig. 5d, and Supplementary Fig. S7C, D). To further investigate whether *AXL* and NR1D2 were in the same pathway in regulating EMT, we performed rescue assay using *AXL*- adenoviruses. To our surprise, *AXL* could partially restore the ability of migration and invasion of GBM cells (Fig. 5a), but could not rescue the expression of Slug and E-cadherin in NR1D2 silencing LN-18 cells (Fig. 5e and Supplementary Fig. S7E). Besides, silencing of *AXL* only downregulated the expression of *NOTCH4* but not *ZEB2*, *TCF7*, *IL11*, and *NOTCH2*, while all of them were downregulated by NR1D2 knockdown (Supplementary Fig. S7F). These data indicate that NR1D2 has more targets other than *AXL* to regulate EMT in GBM cells.

NR1D2 regulates focal adhesion (FA) maturation through FAK-mediated signaling pathway in glioblastoma cells

Due to obvious morphological changes were observed post NR1D2 ablation in LN-18 cells (Supplementary Fig. S1A),

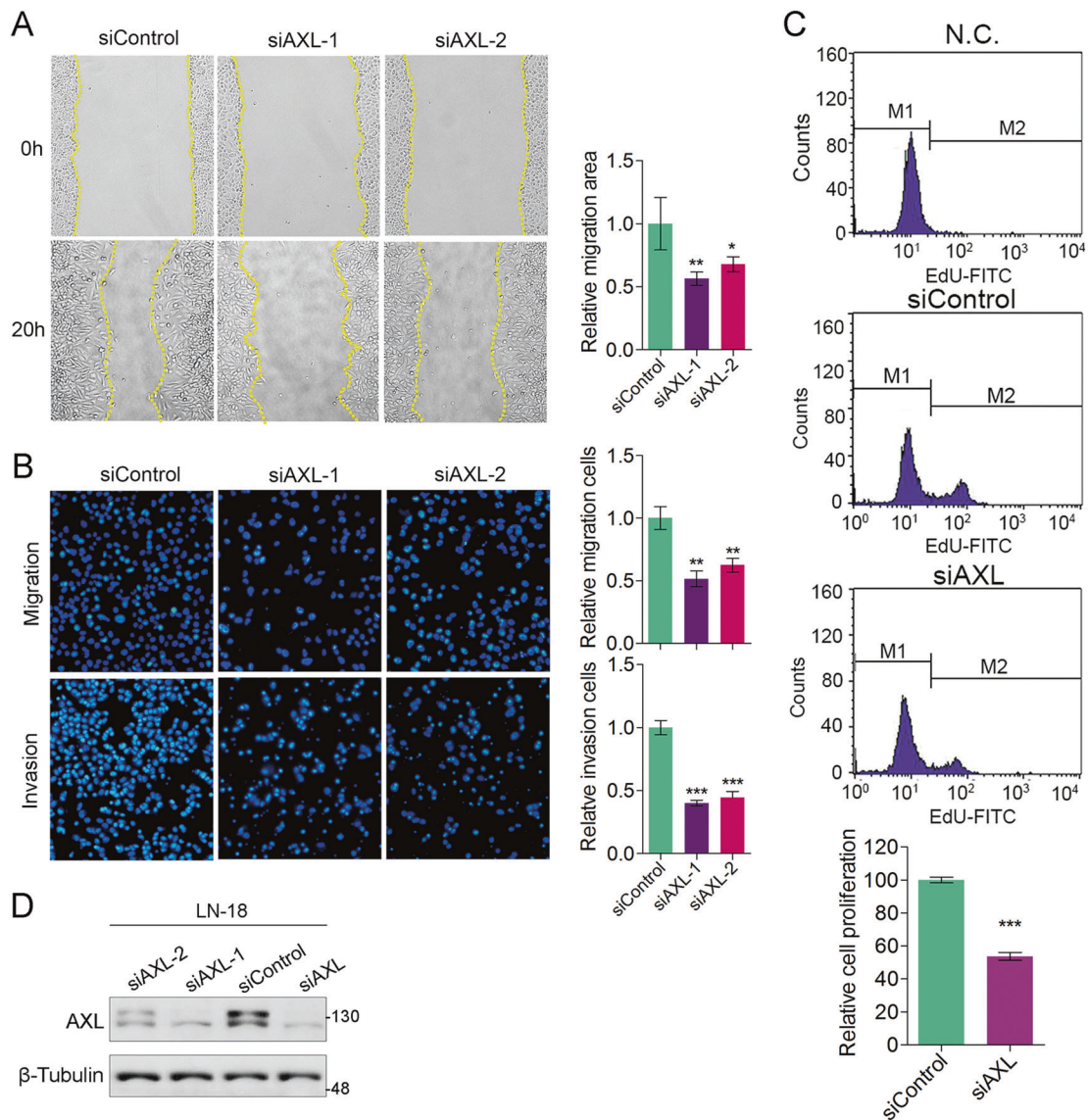


Fig. 3 Inactivation of AXL blocks the proliferation and migration of LN-18 cells. **a** Knockdown of AXL slowed down the migration of LN-18 cells. Wound healing assay was performed on AXL knockdown (AXL-KD) LN-18 cells. Relative scratch covered area was quantified by Image J from four different areas. **b** Inactivation of AXL impaired the ability of cell migration and invasion. Transwell-based cell migration and invasion assay were performed in AXL-KD cells, and matrigel was coated on the bottom of the well as the basement membrane matrix for invasion assay. Migration and invasion cells

were quantified by Image J in 12 random fields from three independent experiments. **c** Knockdown of AXL inhibited cell proliferation. Cell proliferation was measured by EdU incorporation followed with FACS analysis. EdU untreated cells were served as negative control (N.C.). Relative proliferation rate of AXL-KD cells was calculated from triplicates. SiAXL was the mixture of siAXL-1 and siAXL-2. **d** The efficacy of AXL siRNAs was measured by western blotting. Histograms in this figure were shown as means \pm SD (standard derivation). Bars denoted SD. * $P < 0.05$; ** $P < 0.01$; *** $P < 0.001$

which seems to relate to cytoskeleton alteration, and the alteration of focal adhesion signaling pathway (Fig. 4a, b), we carefully monitored cell adhesion related proteins using immunofluorescence. Impaired focal adhesion (FA) was noticed in NR1D2-KD cells by immunostaining of vinculin, a marker for FA (Fig. 6a, d and Supplementary Fig. S8A–C). The sizes of the whole cell and FAs were smaller than that in siControl cells when NR1D2 was knockdown (Fig. 6c, d), whereas knockdown of AXL had negligible

effects on focal adhesion and cell size (Fig. 6c, d). The results suggest that focal adhesion alteration of GBM cells post NR1D2 silencing may be independent of AXL.

FAs were matured from nascent adhesion. FAK is an important mediator in FA signaling pathway and is indispensable for nascent adhesion formation, FA maturation and F-actin assembly (Supplementary Fig. S5) [40–42]. Silencing of NR1D2 obviously decreased the phosphorylated FAK(Y925) even though the total amount of FAK

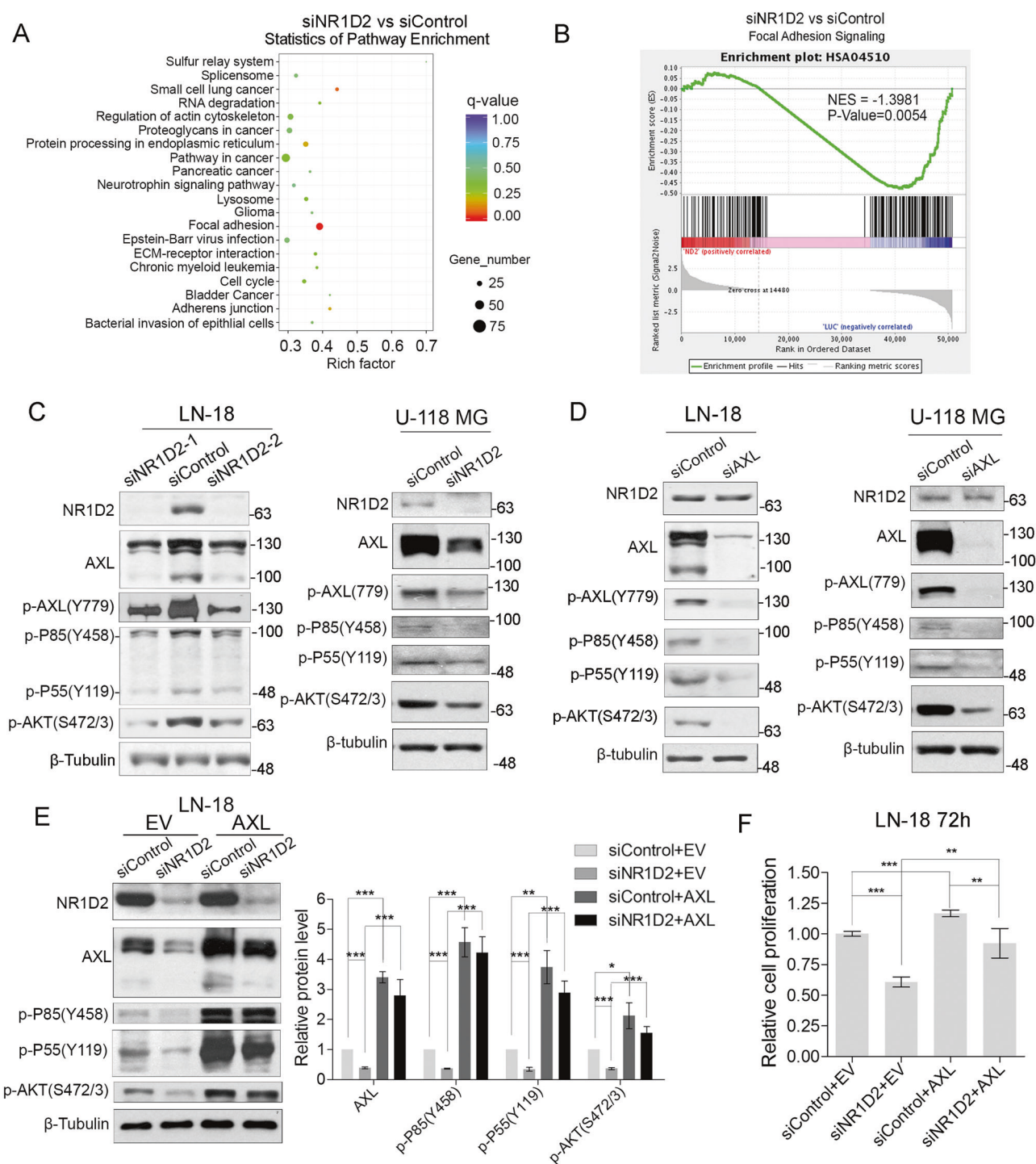


Fig. 4 NR1D2 regulates glioblastoma cells proliferation may through AXL/PI3K/AKT pathway. **a** KEGG scatterplot of DEGs showed significantly altered pathways in NR1D2-KD cells. DEGs, differentially expressed genes. **b** Gene-set enrichment analysis showed the expression changes of genes involved in focal adhesion signaling pathway in NR1D2-KD LN-18 cells. NES, normalized enrichment score. **c–e** NR1D2 regulated RTK-PI3K-AKT pathway mediated by AXL. Representative western blots of AXL-PI3K-AKT pathway members in NR1D2-KD (**c**) and AXL-KD LN-18 cells (**d**). **e** Exogenous expression of AXL in NR1D2-KD LN-18 cells compensated

decreased p-PI3K (P85/P55) and p-AKT. Transfected with indicated siRNAs for 24 h, LN-18 cells were infected by adenoviruses from either pAdm-AXL or empty vector (EV). The proteins were detected using specific antibodies as indicated. Relative protein levels of interest were normalized to β -tubulin and quantified by Image J from triplicates and plotted on the right panel. **f** Exogenous expression of AXL restored cell growth, which was slowed down by silencing of NR1D2. The histogram was generated from three independent experiments. Bars denoted SD. * $P < 0.05$; ** $P < 0.01$; *** $P < 0.001$

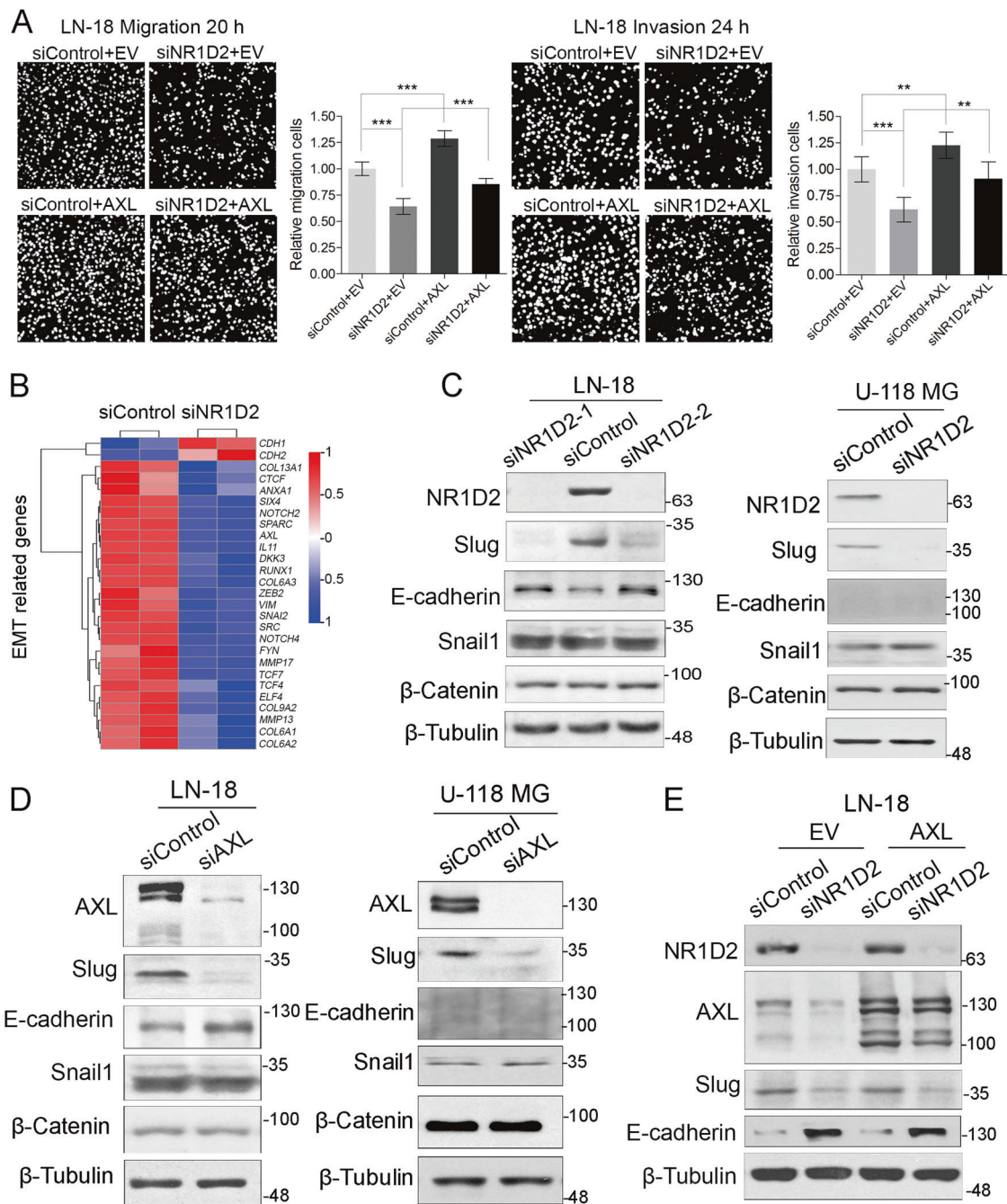
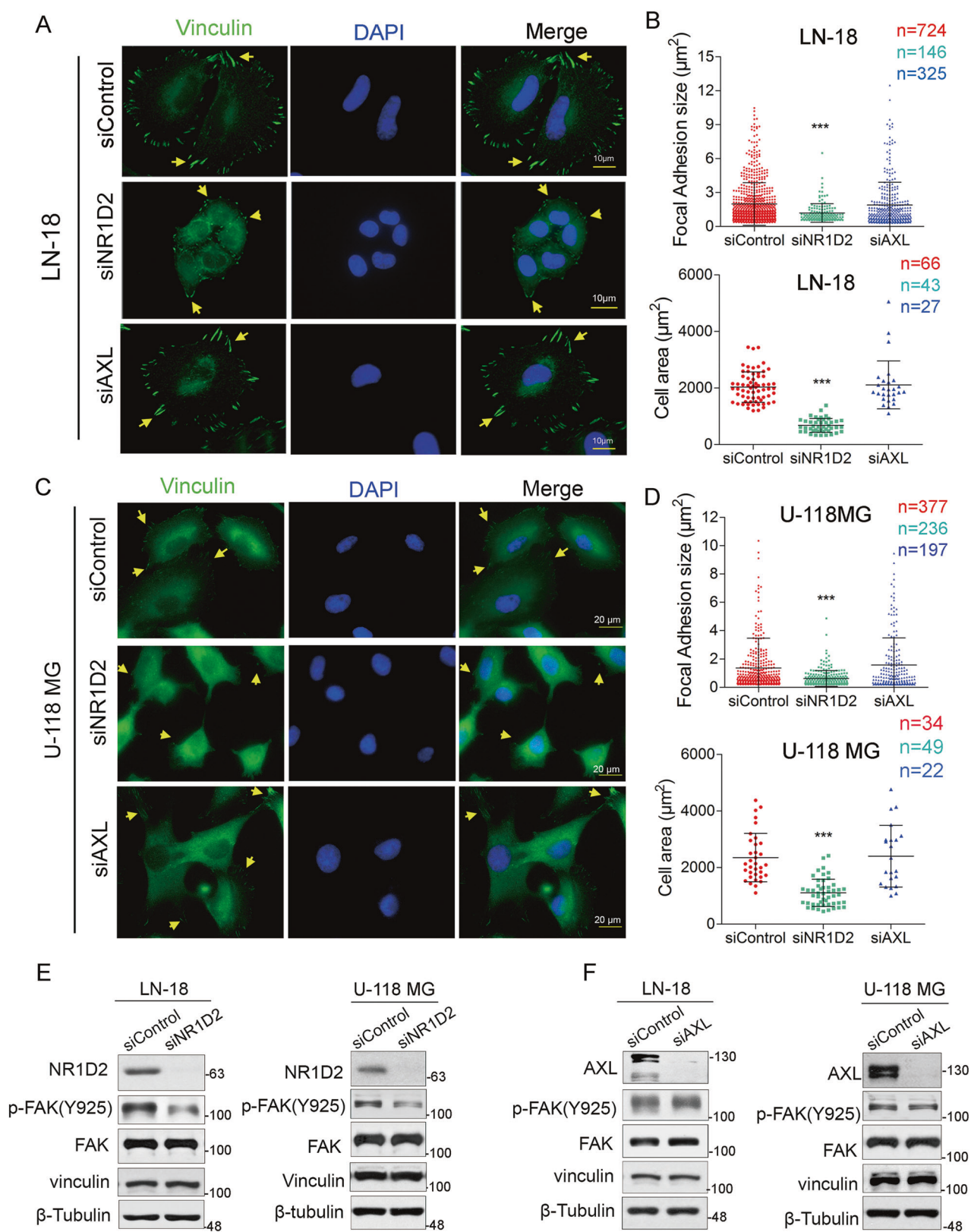


Fig. 5 NR1D2 has more targets other than AXL to regulate EMT in glioblastoma cells. **a** Exogenous expression of AXL stimulated cell migration and invasion. Transwell assay was performed to investigate the rescue effect of AXL in NR1D2-KD LN-18 cells. Matrigel was coated on the bottom of the well as the basement membrane matrix for invasion assay. The migration and invasion cell numbers were quantified by Image J in 12 random fields from three independent experiments. Bars denoted SD. *** $P < 0.001$. **b** Heatmap of EMT-related genes from RNA-seq data in NR1D2-KD LN-18 cells. **c** Knockdown

of NR1D2 altered the expression of EMT-related genes in LN-18 and U-118 MG cells, which was examined by western blotting. The quantification of protein levels was shown in Supplementary Fig. S7A. **d** Silencing of AXL changed the expression of EMT-related genes in LN-18 and U-118 MG cells. The quantification of protein levels was shown in Supplementary Fig. S7D. **e** Exogenous expression of AXL could not rescue the expression of EMT-markers, which was altered in NR1D2-KD cells. The quantification of protein levels was shown in Supplementary Fig. S7E

were kept in constant (Fig. 6e and Supplementary Fig. S8C). Contrary to NR1D2 knockdown, both total FAK and phosphorylated FAK (Y925) remained constant in AXL knockdown cells (Fig. 6f and Supplementary Fig. S8D). To

summarize, our data suggest that NR1D2 regulates FA maturation mediated by FAK signaling pathway, and it is independent of AXL.



◀ **Fig. 6** NR1D2 regulates the formation of focal adhesion. **a–d** The size of focal adhesion (FA) was reduced under NR1D2 siRNAs treatment but not AXL siRNAs treatment. Vinculin (green) was immunostained to indicate formation of FA in LN-18 (**a**) and U-118 MG cells (**c**). DNA was stained by DAPI to represent nuclei. Scale bar: 10 or 20 μm . **b, d** Focal adhesion (FA) and cell size were quantified by Image J and plotted by GraphPad Prism 5.0. Data were shown as means \pm SD. *** $P < 0.001$. **e** NR1D2 regulated FA maturation through p-FAK. Western blotting analysis indicated that the phosphorylation of FAK (Y925) was downregulated by NR1D2 knockdown. The quantification of protein levels of interest was shown in Supplementary Fig. S8C. **f** Knockdown of AXL had negligible effect on p-FAK. The quantification of protein levels of interest was shown in Supplementary Fig. S8D

NR1D2 is indispensable for F-actin polymerization in glioblastoma cells

Since F-actin polymerization is a key event in nascent adhesion formation and cell contraction, we clustered actin regulators from DEGs results (Fig. 7a and Supplementary Table S3) [43]. The protein levels of WAVE2, PFN1, PFN2, and p-Rac1/Cdc42 (S71) were all downregulated post NR1D2 knockdown in LN-18 and U-118 MG cells (Fig. 7b, c and Supplementary Fig. S9). Although p-Rac1/Cdc42 (S71) had a reduction when AXL was knockdown, the protein levels of WAVE2, PFN1, and PFN2 seemed not affected by AXL knockdown (Fig. 7b, c and Supplementary Fig. S9). We had established that NR1D2 was closely related to actin nucleation, polymerization and focal adhesion. On this basis, we performed immunofluorescence in LN-18 and U-118 MG cells with NR1D2 or AXL knockdown. Consistently, the polymerization of F-actin was dependent on NR1D2 but not AXL (Fig. 7d, e). Phalloidin-labeling showed obvious reduction of fibrous actin in NR1D2 knockdown cells but not AXL knockdown cells (Fig. 7d, e). These results suggest that NR1D2 is required for polymerization of F-actin, which may not be mediated by AXL.

Discussion

Both NR1D2 and AXL are indispensable for glioblastoma cell proliferation, migration, and invasion

NR1D2, a ligand-dependent transcriptional repressor for circadian rhythm, metabolism and inflammatory response, is recently found predominantly expressed in various cancers. In this study, we found that NR1D2 was abundantly expressed in glioma tissue and cell lines, consistent with high expression of AXL (Figs. 1a, b and 2c). Ideally, knockdown of NR1D2 or AXL impaired cell proliferation, migration, and invasion (Figs. 1 and 3). Thus, our data

demonstrate that NR1D2 and AXL are indispensable for GBM cell proliferation, migration, and invasion.

AXL is a new target of NR1D2

AXL, a receptor tyrosine kinase (RTK) belonging to the TAM family, is highly expressed in numerous cancers and positively correlated with the mesenchymal phenotype. AXL-mediated EMT also results in drug resistance in neuroblastoma [27, 29]. And the signaling pathways downstream of AXL are cell/tissue type specific in health and disease [28]. In our study, siRNA-mediated knockdown of NR1D2 caused down regulation of AXL, along with its cytomembrane localization ablation (Fig. 2b, d, e). Based on ChIP assay, we confirmed that NR1D2 associated with the upstream region of *AXL* from -304 bp to -467 bp (Fig. 2g). Besides, the regulatory region of *AXL* promoter could be activated by NR1D2 in dual-luciferase reporter system (Fig. 2h). Thereby, our data illustrate that NR1D2 is the activator of AXL.

NR1D2 regulating proliferation and motility of glioblastoma cells partially mediated by AXL via PI3K/AKT signaling pathway

Since AXL was also highly expressed in GBM cells (Fig. 2c) and was indispensable for cells proliferation, migration, and invasion (Fig. 3), we investigated whether AXL was necessary for NR1D2-mediated cells growth and motility. We identify that PI3K/AKT is the major pathway response to NR1D2 or AXL silencing (Fig. 4c, d). Exogenous expression of AXL compensated decrease of phosphorylated PI3K (P85 and P55) and AKT, and restored cell growth (Fig. 4e, f), which was induced by NR1D2 knockdown.

It is well established that the gain of capability for tumor metastasis depends, at least partially, on the acquisition of mesenchymal signatures. We found that silencing of either NR1D2 or AXL impaired epithelial-to mesenchymal transition in glioblastoma cells (Fig. 5a–d). Exogenous expression of AXL partially restored the capability of cell migration and invasion in siRN1D2 cells, although did not affect the changes of Slug and E-cadherin altered by NR1D2 depletion (Fig. 5a, e). Also, knockdown of AXL only reduced the expression of NOTCH4 but not ZEB2, TCF7, IL11 and NOTCH2, while all of them were decreased post NR1D2 knockdown (Supplementary Fig. S7F). These data demonstrate that NR1D2 has more targets other than AXL to regulate EMT in GBM cells. Overall, our data illustrate that AXL mediates the partial promotion effects of NR1D2 via PI3K/AKT axis on cell proliferation, migration, and invasion in GBM.

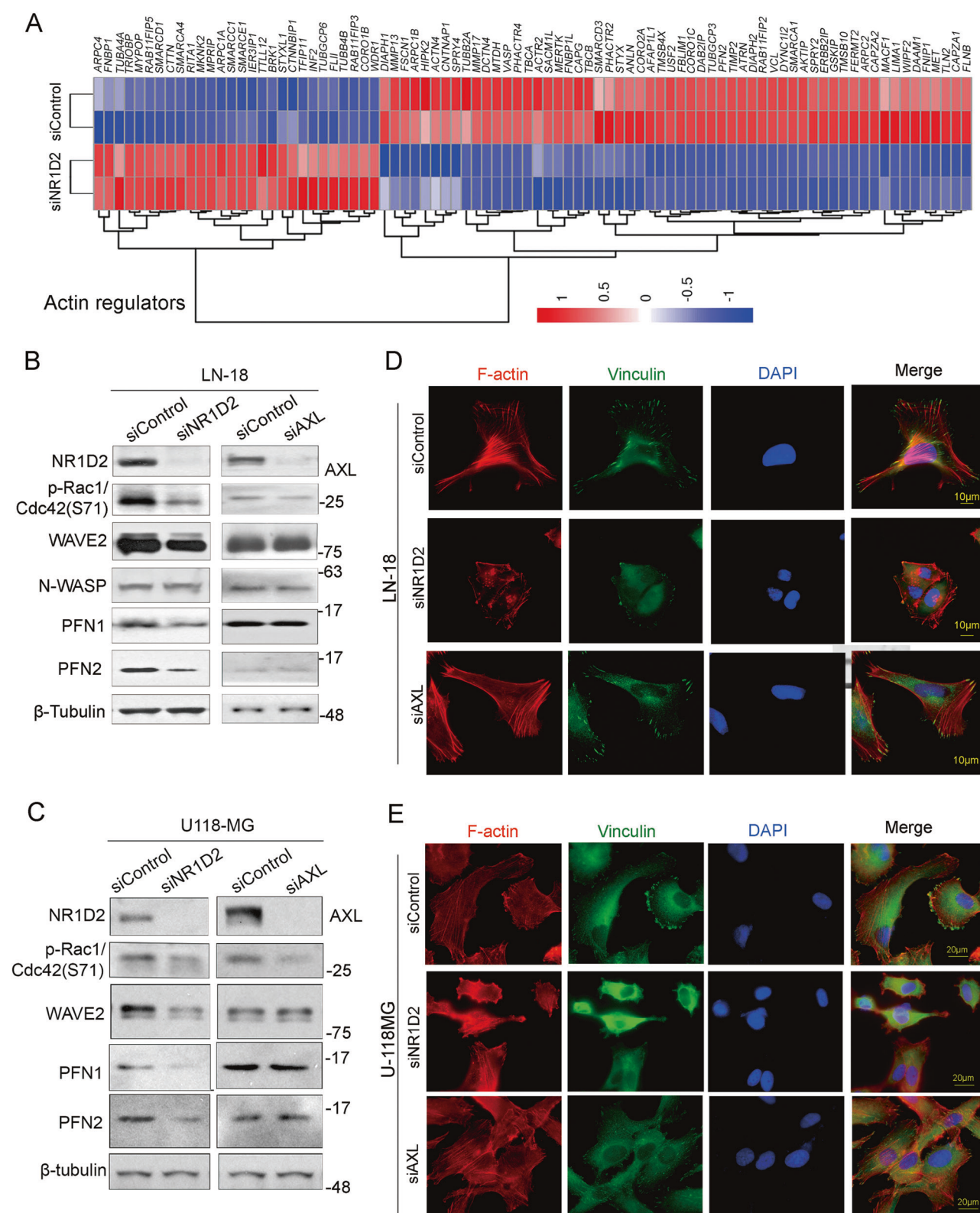


Fig. 7 NR1D2 regulates the polymerization of F-actin. **a** Heatmap displayed the expression levels of actin regulators in NR1D2-KD LN-18 cells. **b, c** Western blotting analysis of actin nucleation and polymerization correlated proteins in NR1D2 knockdown and AXL knockdown LN-18 and U-118 MG cells. The quantification of protein

levels of interest was shown in Supplementary Fig. S9. **d, e** NR1D2 regulated the assembly of F-actin independent of AXL. Immunofluorescence was carried out to display F-actin (phalloidin, red), FA (vinculin, green) and nuclei (DAPI, blue) in siControl, siNR1D2 or siAXL-treated LN-18 and U-118 MG cells. Scale bar: 10 μ m

NR1D2 regulates FA maturation and F-actin polymerization in glioblastoma cells

Actin nucleation and polymerization are essential processes for actin assembly and cytoskeleton construction, which is the fundamental for cancer cell spreading, migration and metastasis. KEGG enrichment analysis of DEGs in RNA-seq finally focused on the focal adhesion signaling pathway (Fig. 4a and Supplementary Fig. S5), a complicated pathway involves in cell motility, cell proliferation, and cell survival, and regulated by numerous vital factors, such as RTK, PKC, PI3K, AKT, WNT, MAPK, MEK1, Rac1 et al. (Supplementary Fig. S5). Among the DEGs, most of the actin regulators were downregulated, such as WAVE2, PFN1, and PFN2 (Fig. 7a), which was confirmed at the protein level (Fig. 7b, c and Supplementary Fig. S9). Inhibition of NR1D2 severely impaired F-actin assembly and FA maturation (Figs. 6 and 7), caused cell shrinking (Supplementary Fig. S1A, B), subsequently disable glioma cell to move (Fig. 1c, d and Supplementary Fig. S2C, D), and the major cause was suggested from dysregulation of phosphorylated FAK and Rac1 (Figs. 6e and 7b, c). Although being a target of NR1D2, AXL seemed not involved in (Figs. 6 and 7b–e). Taken together, NR1D2 has broader downstream targets other than AXL, and regulates FA maturation and F-actin polymerization.

NR1D2 may be a novel target for glioblastoma therapy

GBM remains one of the most challenging malignancies worldwide. No early detection of GBM is available and the results from clinical trials of novel therapeutic approaches and drugs are disappointing. The somatic alterations in GBM are major involved in the RB, TP53, and RTK pathways [1], and ~74% aberrations are in all three pathways and ~88% of GBM harbor at least one genetic event in the RTK/PI3K pathway [44].

Our data demonstrate that NR1D2 is highly expressed in GBM, directly regulates AXL expression, is required for cell proliferation, epithelial-to mesenchymal transition, focal adhesion maturation, and F-actin polymerization, which is related to cell migration and invasion, and may mediated by AXL/PI3K/AKT or FAK pathways. In view of NR1D2 is predominant in various cancers and its homolog variant NR1D1 is prevailing in normal tissues, it suggests NR1D2 might be a novel target for GBM therapy.

Materials and methods

Cell lines

Human glioblastoma cell lines LN-18, T98G, U-87 MG, U-118 MG, and HCT116 were purchased from American Type Cell Collection (ATCC). Human astrocytes (HA) was purchased from China Infrastructure of Cell Line Resource. U-373 MG was a gift from Dr. Hui Zhang (Department of Chemistry and Biochemistry, University of Nevada, Las Vegas, NV 89154, USA). All cells were maintained in Dulbecco's Modified Eagle Medium (DMEM) with 10% fetal bovine serum (FBS), 100 U/mL penicillin and 100 µg/mL streptomycin at 37 °C, 5% CO₂ incubator. HA was additionally supplemented with N-2 Supplement (100x). All cells were authenticated and tested clear of mycoplasma contamination.

siRNAs and transfection

For siRNA-mediated gene silencing, cells were transfected with 50 nM siRNAs for 36–72 h using DharmaFECT Transfection Reagent (#T-2001-03, ThermoFisher Scientific Inc.) according to the product manual. To rule out potential off-target effects of siRNAs, at least two pairs of siRNAs for each gene were designed. All siRNA experiments were repeated at least three times to obtain the consistent results. The sequences for siRNAs were as follows: Control: 5'-UUCUCCGAACGUGUCACGU-3', NR1D2-1: 5'-GGGAGGAAUUAUAUGCAUU-3', NR1D2-2: 5'-GCACUAAGGACCUUAAUAA-3', AXL-1: 5'-ACAUAGGGCUAAGGCAAGA-3', AXL-2: 5'-ACAGCGAGAUUUAUGACUA-3'.

RNA-seq and RT-qPCR

Total RNA was extracted using RNAiso Plus (#9109, Takara Biomedical Technology). RNA-seq was carried out by Novogene Bioinformatics Technology Co., Ltd (Beijing, China). RNA-seq was performed in duplicate. The list of DEGs were available in Supplementary Table S1 and S2.

For RT-qPCR, total RNA was used to generate cDNA by reverse transcriptase M-MLV (RNase H) (#2641A, Takara Biomedical Technology). The mRNA levels of target genes were quantified using SYBR Fast qPCR Mix (#RR430S, Takara Biomedical Technology) in a CFX Connect Real-Time PCR Detection System (#1855200, Bio-Rad Laboratories, Inc.). β-Actin was taken for normalization. The sequences for primers were listed in Supplementary Table S4.

Chromatin immunoprecipitation (ChIP)

ChIP assays were performed as described [45] in LN-18 cells with purified anti-NR1D2 antibody, and rabbit IgG was taken as negative control. Briefly, proteins were cross-linked to DNA by formaldehyde (0.75%). Cells were harvested and sonicated to generate DNA fragments of ~500 bp in average. Soluble chromatin fragments were incubated with primary antibodies overnight. Purified DNA was used for qPCR to detect the binding sites of NR1D2. GAPDH was taken for normalization. The sequences for primers were listed in Supplementary Table S5.

Immunofluorescence

After transfected for 36–48 h, cells were resuspended and reseeded on glass slides 24 h prior to the experiments. Fixed with 4% paraformaldehyde for 20 min, cells were washed twice with PBS and permeabilized with 0.5% Triton X-100, followed by blocking with 3% BSA for 1 h. Cellular targets were incubated with primary antibodies at 4 °C overnight. After washed with PBS, incubated with FITC or TRITC-conjugated secondary antibodies at room temperature for 1–2 h, and sequentially incubated with Rhodamine Phalloidin (R415, ThermoFisher Scientific) at room temperature for 30 min, cells were mounted with mowiol (sigma) containing 1 µg/mL DAPI. Images were captured on an Olympus fluorescence microscope (Olympus CKX41, Japan) coupled to a cooled charge-coupled device camera (QICAM, Japan) and processed using the QCapture Pro 6.0 program.

Wound healing, cell migration, and invasion assay

Images of wounds were captured at 0 and 20 (or 16) hours after scratching with a sterile 10 µL pipette. The coverage of the scratched area was measured at four different positions by Image J. Triplicates were performed to obtain consistent results.

Cell migration and invasion assays were carried out using Boyden chambers containing membrane filter inserts with a pore size of 8 µm (Corning, NY). For the invasion assay, diluted Matrigel (BD Biosciences) was used. Forty-eight hours post transfection, 20,000–40,000 cells were seeded on the top chamber supplemented with 100 µL DMEM without FBS, and the bottom chamber was filled with 500 µL DMEM containing 10% FBS. After incubated for 12–24 h at 37 °C, the top chamber was removed, and unigrated cells were gently scraped. The migrated cells were fixed with 4% paraformaldehyde for 20 min and washed twice with PBS. Nuclei were stained with 1 µg/mL DAPI and randomly counted under the microscope.

Dual-luciferase reporter assay

The cDNA of full-length NR1D2 was inserted into p3 × FLAG-CMV10 with *Hind*III and *Eco*RI digestion. The fragment of *AXL* promoter (–177~–600bp) was amplified from human genome and cloned into pGL3 luciferase reporter vectors with *Kpn*I and *Xho*I digestion. The pGL3-*AXL* promoter, pRL-TK (containing the Renilla luciferase reporter), and p3 × FLAG-CMV10 (Control) or p3 × FLAG-CMV10-NR1D2 were co-transfected into HCT116 cells. Forty-eight hours later, luciferase activity was measured using the Dual-Luciferase® Reporter Assay System (E1910, Promega) according to the product manual. The value of firefly luciferase activity was normalized to that of the Renilla activity. The primers used were: NR1D2_forward: 5'- CCCAAGCTTATGGAGGTGAATGCAGGAGGT-3', NR1D2_reverse: 5'- CCCGAATTCTTAAGGGTGAACCTTAAAGGCC-3', *AXL* promoter_forward: 5'- TGCGGTA CCGTGTGTGTGTGTCCTTGTC-3', *AXL* promoter_reverse: 5'- ATACTCGAGCTGCCTCCTTCCCTCACTC-3'.

Antibodies

Anti-NR1D2 antibody was home-made using fragment of GST-NR1D2 (268–379 aa) as antigen and purified by protein A coupled-sepharose resins. Anti-*AXL* (8661S), WAVE2 (8606T), p-FAK (Y925) (3284T), PFN1 (8606T), p-Rac1/Cdc42(S71) (8606T), N-WASP (8606T), and p-PI3K-p85 (Tyr458)/p55 (Tyr199) (4228S) antibodies were purchased from Cell Signaling Technology (Danvers, MA), anti-PFN2 (60094-2-Ig), FAK (12636-1-AP), SNAI1 (13099-1-AP), E-Cadherin (20874-1-AP), β-catenin (51067-2-AP), β-tubulin (66240-1-Ig), and Flag (20543-1-AP) antibodies were from Proteintech Group (Wuhan, China). Anti-Vinculin (ab73412) antibody was from Abcam (Shanghai, China), anti-p-*AXL*(Y779) (AF2228) antibody was from R&D Systems (Minneapolis, MN), anti-p-AKT (S472/473) (550747), Slug (564614) antibodies were from BD Biosciences (Shanghai, China). FITC or TRITC-conjugated secondary antibodies were from Jackson ImmunoResearch Inc. (West Grove, PA).

Cell cycle analysis and EdU labeling

The fluorescence-activated cell sorting (FACS) and 5-ethynyl-20-deoxyuridine (EdU) labeling were conducted as described previously [46]. Click-iT EdU Alexa Fluor 488 Flow Cytometry Assay Kit (C10425) was purchased from ThermoFisher Scientific Inc. In brief, after transfected with indicated siRNAs for 70 h and then incubated with EdU for half an hour, LN-18 cells were harvested and fixed for the assay according to the product manual.

Immunohistochemistry (IHC) and tissue RNA isolation

IHC was performed using HRP/DAB (ABC) detection IHC Kit (ab64261, Abcam) and approved by Medical Ethics Committee of Qingdao Municipal Hospital. Briefly, all available paraffin-embedded tissue sections of glioma were obtained from Qingdao Municipal Hospital, Qingdao University. The sections were deparaffinized, rehydrated, and immersed in 3% H₂O₂/methanol for 10 min at room temperature to inactivate endogenous peroxidase. Antigens were heat-retrieved in sodium citrate buffer (10 mM sodium citrate, 0.05% Tween 20, pH 6.0) at 100 °C for 8 min. After blocked for 20 min, tissues were incubated with rabbit anti-NR1D2 antibody at a dilution of 1:150 overnight at 4 °C. Then the sections were washed, incubated with biotinylated goat anti-polyvalent antibody, DAB Chromogen and Substrate, and counter stained following manufacturer's protocol. Images were captured under the microscope.

Tissue RNA isolation was carried out using FFPE RNA Kit (R6954, Omega Bio-Tek) according to the product manual. Isolated total RNA was quantified and used to generate cDNA by reverse transcriptase M-MLV. The mRNA level of NR1D2 was quantified by real-time PCR.

Gene-set enrichment analysis (GESA)

GESA 2.0. was run to analyze gene sets that were functional related to focal adhesion signaling pathway, which were obtained from published gene signatures, and statistical significance was assessed as described [47].

Statistical analysis

All experiments were biologically repeated at least three times, and only one set was presented. The data used for statistical analysis were all in normal distribution. The statistical data were presented as mean ± SD (standard derivation) from three different biological repeats or technique repeats as mentioned in Figure Legends. The paired two-tailed student's *t*-test were performed to determine statistical significance between experimental group and control group, and $P < 0.05$ was considered as significant. *denotes $P < 0.05$, ** denotes $P < 0.01$, ***denotes $P < 0.001$. Image J and GraphPad Prism (version 5.0) were used for data analysis and plots generation.

Acknowledgements This work was supported by grants from Natural Science Foundation of Guangdong Province (grant no. 2014A030313779), Shenzhen basic research program (grant no. JCYJ20160527100529884 and JCYJ20170818085657917). We thank Dr. Hui Zhang for the kind gift of U-373 MG cell line.

Author contributions F.L. and M.Y. perceived the conception, analyzed the findings, and wrote the manuscript; M.Y. executed most of the experiments. W.L., Q.W. assisted in execution of some experiments, and Y.W. provided tumor specimens. All authors reviewed the results and approved the final version of the manuscript.

Compliance with ethical standards

Conflict of interest The authors declare that they have no conflict of interest.

References

- Brennan CW, Verhaak RG, McKenna A, Campos B, Noushmehr H, Salama SR, et al. The somatic genomic landscape of glioblastoma. *Cell*. 2013;155:462–77.
- Alexander BM, Cloughesy TF. Adult glioblastoma. *J Clin Oncol: Off J Am Soc Clin Oncol*. 2017;35:2402–9.
- Stupp R, Hegi ME, Neyns B, Goldbrunner R, Schlegel U, Clement PM, et al. Phase I/IIa study of cilengitide and temozolomide with concomitant radiotherapy followed by cilengitide and temozolomide maintenance therapy in patients with newly diagnosed glioblastoma. *J Clin Oncol: Off J Am Soc Clin Oncol*. 2010;28:2712–8.
- Gilbert MR, Dignam JJ, Armstrong TS, Wefel JS, Blumenthal DT, Vogelbaum MA, et al. A randomized trial of bevacizumab for newly diagnosed glioblastoma. *N Engl J Med*. 2014;370:699–708.
- Gilbert MR, Pugh SL, Aldape K, Sorensen AG, Mikkelsen T, Penas-Prado M, et al. NRG oncology RTOG 0625: a randomized phase II trial of bevacizumab with either irinotecan or dose-dense temozolomide in recurrent glioblastoma. *J Neurooncol*. 2017;131:193–9.
- Weathers SP, Han X, Liu DD, Conrad CA, Gilbert MR, Lohin ME, et al. A randomized phase II trial of standard dose bevacizumab versus low dose bevacizumab plus lomustine (CCNU) in adults with recurrent glioblastoma. *J Neurooncol*. 2016;129:487–94.
- Wick W, Gorlia T, Bady P, Platten M, van den Bent MJ, Taphoorn MJ, et al. Phase II study of radiotherapy and temsirinolimus versus radiochemotherapy with temozolomide in patients with newly diagnosed glioblastoma without MGMT promoter hypermethylation (EORTC 26082). *Clin Cancer Res: Off J Am Assoc Cancer Res*. 2016;22:4797–806.
- Chamberlain MC, Kim BT. Nivolumab for patients with recurrent glioblastoma progressing on bevacizumab: a retrospective case series. *J Neurooncol*. 2017;133:561–9.
- Iser IC, Pereira MB, Lenz G, Wink MR. The epithelial-to-mesenchymal transition-like process in glioblastoma: An updated systematic review and in silico investigation. *Med Res Rev*. 2017;37:271–313.
- Eddleston M, Mucke L. Molecular profile of reactive astrocytes—implications for their role in neurologic disease. *Neuroscience*. 1993;54:15–36.
- Wong GS, Rustgi AK. Matricellular proteins: priming the tumour microenvironment for cancer development and metastasis. *Br J Cancer*. 2013;108:755–61.
- Meng J, Li P, Zhang Q, Yang Z, Fu S. A radiosensitivity gene signature in predicting glioma prognostic via EMT pathway. *Oncotarget*. 2014;5:4683–93.
- Mahabir R, Tanino M, Elmansuri A, Wang L, Kimura T, Itoh T, et al. Sustained elevation of Snail promotes glial-mesenchymal transition after irradiation in malignant glioma. *Neuro Oncol*. 2014;16:671–85.

14. Kubelt C, Hattermann K, Sebens S, Mehdorn HM, Held-Feindt J. Epithelial-to-mesenchymal transition in paired human primary and recurrent glioblastomas. *Int J Oncol*. 2015;46:2515–25.
15. Yan YR, Xie Q, Li F, Zhang Y, Ma JW, Xie SM, et al. Epithelial-to-mesenchymal transition is involved in BCNU resistance in human glioma cells. *Neuropathol: Off J Jpn Soc Neuropathol*. 2014;34:128–34.
16. Hutterer M, Knyazev P, Abate A, Reschke M, Maier H, Stefanova N, et al. Axl and growth arrest-specific gene 6 are frequently overexpressed in human gliomas and predict poor prognosis in patients with glioblastoma multiforme. *Clin Cancer Res: Off J Am Assoc Cancer Res*. 2008;14:130–8.
17. Verma A, Warner SL, Vankayalapati H, Bears DJ, Sharma S. Targeting Axl and Mer kinases in cancer. *Mol Cancer Ther*. 2011;10:1763–73.
18. Rankin EB, Giaccia AJ. The receptor tyrosine kinase AXL in cancer progression. *Cancers*. 2016;8:16.
19. Wilson C, Ye X, Pham T, Lin E, Chan S, McNamara E, et al. AXL inhibition sensitizes mesenchymal cancer cells to antimetabolic drugs. *Cancer Res*. 2014;74:5878–90.
20. Vuoriluoto K, Haugen H, Kiviluoto S, Mpindi JP, Nevo J, Gjerdrum C, et al. Vimentin regulates EMT induction by Slug and oncogenic H-Ras and migration by governing Axl expression in breast cancer. *Oncogene*. 2011;30:1436–48.
21. Byers LA, Diao L, Wang J, Saintigny P, Girard L, Peyton M, et al. An epithelial-mesenchymal transition gene signature predicts resistance to EGFR and PI3K inhibitors and identifies Axl as a therapeutic target for overcoming EGFR inhibitor resistance. *Clin Cancer Res: Off J Am Assoc Cancer Res*. 2013;19:279–90.
22. Asiedu MK, Beauchamp-Perez FD, Ingle JN, Behrens MD, Radisky DC, Knutson KL. AXL induces epithelial-to-mesenchymal transition and regulates the function of breast cancer stem cells. *Oncogene*. 2014;33:1316–24.
23. Vajkoczy P, Knyazev P, Kunkel A, Capelle HH, Behrndt S, von Tengg-Kobligk H, et al. Dominant-negative inhibition of the Axl receptor tyrosine kinase suppresses brain tumor cell growth and invasion and prolongs survival. *Proc Natl Acad Sci USA*. 2006;103:5799–804.
24. Zhang Z, Lee JC, Lin L, Olivas V, Au V, LaFramboise T, et al. Activation of the AXL kinase causes resistance to EGFR-targeted therapy in lung cancer. *Nat Genet*. 2012;44:852–60.
25. Varnum BC, Young C, Elliott G, Garcia A, Bartley TD, Fridell YW, et al. Axl receptor tyrosine kinase stimulated by the vitamin K-dependent protein encoded by growth-arrest-specific gene 6. *Nature*. 1995;373:623–6.
26. Bellosta P, Costa M, Lin DA, Basilico C. The receptor tyrosine kinase ARK mediates cell aggregation by homophilic binding. *Mol Cell Biol*. 1995;15:614–25.
27. Zhou L, Liu XD, Sun M, Zhang X, German P, Bai S, et al. Targeting MET and AXL overcomes resistance to sunitinib therapy in renal cell carcinoma. *Oncogene*. 2016;35:2687–97.
28. Axelrod H, Pienta KJ. Axl as a mediator of cellular growth and survival. *Oncotarget*. 2014;5:8818–52.
29. Debruyne DN, Bhatnagar N, Sharma B, Luther W, Moore NF, Cheung NK, et al. ALK inhibitor resistance in ALK(F1174L)-driven neuroblastoma is associated with AXL activation and induction of EMT. *Oncogene*. 2016;35:3681–91.
30. Forman BM, Chen J, Blumberg B, Kliewer SA, Henshaw R, Ong ES, et al. Cross-talk among ROR alpha 1 and the Rev-erb family of orphan nuclear receptors. *Mol Endocrinol*. 1994;8:1253–61.
31. Raghuram S, Stayrook KR, Huang P, Rogers PM, Nosie AK, McClure DB, et al. Identification of heme as the ligand for the orphan nuclear receptors REV-ERBalpha and REV-ERBbeta. *Nat Struct Mol Biol*. 2007;14:1207–13.
32. Ramakrishnan SN, Lau P, Crowther LM, Cleasby ME, Millard S, Leong GM, et al. Rev-erb beta regulates the Srebp-1c promoter and mRNA expression in skeletal muscle cells. *Biochem Biophys Res Commun*. 2009;388:654–9.
33. Preitner N, Damiola F, Lopez-Molina L, Zakany J, Duboule D, Albrecht U, et al. The orphan nuclear receptor REV-ERBalpha controls circadian transcription within the positive limb of the mammalian circadian oscillator. *Cell*. 2002;110:251–60.
34. Cho H, Zhao X, Hatori M, Yu RT, Barish GD, Lam MT, et al. Regulation of circadian behaviour and metabolism by REV-ERB-alpha and REV-ERB-beta. *Nature*. 2012;485:123–7.
35. Raspe E, Duez H, Gervois P, Fievet C, Fruchart JC, Besnard S, et al. Transcriptional regulation of apolipoprotein C-III gene expression by the orphan nuclear receptor RORalpha. *J Biol Chem*. 2001;276:2865–71.
36. Ramakrishnan SN, Lau P, Burke LJ, Muscat GE. Rev-erbbeta regulates the expression of genes involved in lipid absorption in skeletal muscle cells: evidence for cross-talk between orphan nuclear receptors and myokines. *J Biol Chem*. 2005;280:8651–9.
37. Lam MT, Cho H, Lesch HP, Gosselin D, Heinz S, Tanaka-Oishi Y, et al. Rev-Erbs repress macrophage gene expression by inhibiting enhancer-directed transcription. *Nature*. 2013;498:511–5.
38. De Mei C, Ercolani L, Parodi C, Veronesi M, Lo Vecchio C, Bottegoni G, et al. Dual inhibition of REV-ERBbeta and autophagy as a novel pharmacological approach to induce cytotoxicity in cancer cells. *Oncogene*. 2015;34:2597–608.
39. Ott M, Litzemberger UM, Sahm F, Rauschenbach KJ, Tudoran R, Hartmann C, et al. Promotion of glioblastoma cell motility by enhancer of zeste homolog 2 (EZH2) is mediated by AXL receptor kinase. *PLoS ONE*. 2012;7:e47663.
40. Li SY, Mruk DD, Cheng CY. Focal adhesion kinase is a regulator of F-actin dynamics: New insights from studies in the testis. *Spermatogenesis*. 2013;3:e25385.
41. McLean GW, Carragher NO, Avizienyte E, Evans J, Brunton VG, Frame MC. The role of focal-adhesion kinase in cancer - a new therapeutic opportunity. *Nat Rev Cancer*. 2005;5:505–15.
42. Sun Z, Guo SS, Fassler R. Integrin-mediated mechanotransduction. *J Cell Biol*. 2016;215:445–56.
43. Siripala AD, Welch MD. SnapShot: actin regulators I. *Cell*. 2007;128:626.
44. Cancer Genome Atlas Research N. Comprehensive genomic characterization defines human glioblastoma genes and core pathways. *Nature*. 2008;455:1061–8.
45. Yin F, Lan R, Zhang X, Zhu L, Chen F, Xu Z, et al. LSD1 regulates pluripotency of embryonic stem/carcinoma cells through histone deacetylase 1-mediated deacetylation of histone H4 at lysine 16. *Mol Cell Biol*. 2014;34:158–79.
46. Qi D, Wang Q, Yu M, Lan R, Li S, Lu F. Mitotic phosphorylation of SOX2 mediated by Aurora kinase A is critical for the stem-cell like cell maintenance in PA-1 cells. *Cell Cycle*. 2016;15:2009–18.
47. Subramanian A, Tamayo P, Mootha VK, Mukherjee S, Ebert BL, Gillette MA, et al. Gene-set enrichment analysis: a knowledge-based approach for interpreting genome-wide expression profiles. *Proc Natl Acad Sci USA*. 2005;102:15545–50.